Controlling the Range of Interactions in the Classical Inertial Ferromagnetic Heisenberg Model: Analysis of Metastable States

Leonardo J. L. Cirto[1],* Leonardo S. Lima[2],† and Fernando D. Nobre[1,3]‡

[1] *Centro Brasileiro de Pesquisas Físicas, Rua Dr. Xavier Sigaud 150, 22290-180 Rio de Janeiro - RJ, Brazil*

[2] *Departamento de Física e Matemática, Centro Federal de Educação Tecnológica de Minas Gerais, 30510-000 Belo Horizonte - MG, Brazil and*

[3] *National Institute of Science and Technology for Complex Systems, Rua Dr. Xavier Sigaud 150, 22290-180 Rio de Janeiro - RJ, Brazil*

A numerical analysis of a one-dimensional Hamiltonian system, composed by N classical localized Heisenberg rotators on a ring, is presented. A distance r_{ij} between rotators at sites i and j is introduced, such that the corresponding two-body interaction decays with r_{ij} as a power-law, $1/r_{ij}^{\alpha}$ ($\alpha \geq 0$). The index α controls the range of the interactions, in such a way that one recovers both the fully-coupled (i.e., mean-field limit) and nearest-neighbour-interaction models in the particular limits $\alpha = 0$ and $\alpha \to \infty$, respectively. The dynamics of the model is investigated for energies U below its critical value ($U < U_c$), with initial conditions corresponding to zero magnetization. The presence of quasi-stationary states (QSSs), whose durations $t_{\rm QSS}$ increase for increasing values of N, is verified for values of α in the range $0 \leq \alpha < 1$, like the ones found for the similar model of XY rotators. Moreover, for a given energy U, our numerical analysis indicates that $t_{\rm QSS} \sim N^{\gamma}$, where the exponent γ decreases for increasing α in the range $0 \leq \alpha < 1$, and particularly, our results suggest that $\gamma \to 0$ as $\alpha \to 1$. The growth of $t_{\rm QSS}$ with N could be interpreted as a breakdown of ergodicity, which is shown herein to occur for any value of α in this interval.

I. INTRODUCTION

Classical spin models have called the attention of statistical-mechanics and magnetism researchers throughout many years [1–5]. Many techniques have been used in their study, both analytical and numerical, in such a way that a reasonable knowledge of their equilibrium thermodynamics has been achieved, and specially, of their critical properties. Among those models, one could mention the n-vector classical spin models, which present the XY ($n = 2$) and Heisenberg ($n = 3$) as particular cases.

An interesting formulation of a n-vector classical model comes when one adds a kinetic term to its Hamiltonian, i.e., the spin variables may be interpreted as classical rotators (see, e.g., Refs. [6–8]), so that the terminology "inertial model" is currently used. This additional term does not pose difficulties in the calculation of equilibrium properties within a canonical-ensemble approach, but it turns possible to derive equations of motion for each rotator, which can be integrated by means of a molecular-dynamics procedure. In this way, the dynamical behaviour of these models can be investigated numerically without the need of introducing any particular type of probabilistic transition rules for changing the microscopic states.

The inertial ferromagnetic XY model was introduced in Ref. [6], within a fully-coupled framework

*Electronic address: cirto@cbpf.br

†Electronic address: lslima@des.cefetmg.br

‡Electronic address: fdnobre@cbpf.br

(i.e., infinite-range interactions), a limit where the mean-field approach becomes exact. Mostly referred to as "Hamiltonian Mean Field" (HMF) model, it became paradigmatic in the study of the dynamical behaviour of classical many-body Hamiltonian systems, and it has given rise to a large amount of works [9–18]. One of the most interesting features in the HMF model concerns the appearance of metastable states, for some particular initial conditions, whose lifetime grows by increasing the total number of rotators, that could be interpreted as a breakdown of ergodicity in the thermodynamic limit.

A generalization of the HMF model was proposed in Ref. [7], by introducing a distance r_{ij} between rotators at sites i and j of a given lattice. Moreover, the two-body interaction was assumed to decay with r_{ij}, like a power-law, $1/r_{ij}^{\alpha}$ ($\alpha \geq 0$). The index α controls the range of the interactions, in such a way that one recovers both the HMF and nearest-neighbour-interaction models in the particular limits $\alpha = 0$ and $\alpha \to \infty$, respectively. In between these two limits, one finds an important change of behaviour in the thermodynamic quantities, yielding two physically distinct regimes, namely, the long- ($\alpha \leq d$) and short-range ($\alpha > d$) interaction regimes [7, 19–21]. In the latter, one has the usual extensive and intensive quantities, whereas in the former, one may find also nonextensive thermodynamic quantities [22]. This generalization is usually referred to as α-XY or α-HMF model, and it also has been studied by several groups [17, 20, 21, 23–25].

The dynamics of the fully-coupled inertial version of the ferromagnetic Heisenberg model has been much less investigated in the literature [8, 26, 27]. Metastable, or quasi-stationary states (QSSs), also occur for this system, similar to those that appear in the HMF model; their lifetime diverge by increasing the total number of rotators N, which implies that the order in which the thermodynamic limit ($N \to \infty$) and the infinite-time limit ($t \to \infty$) are considered, becomes important. More specifically, if we let $N \to \infty$ first, the system remains trapped in these QSSs, never reaching the final Boltzmann-Gibbs (BG) equilibrium state, most probably being the QSS itself the final state in such a case. In these metastable states, thermodynamical quantities, like temperature and magnetization, do not coincide with the canonical-ensemble predictions.

Herein, we will modify the fully-coupled inertial ferromagnetic Heisenberg model, by introducing a distance r_{ij} between rotators at sites i and j of a given lattice. Analogously to the α-HMF model [7], the rotator-rotator interaction will be taken to decay with the distance like a power-law, $1/r_{ij}^{\alpha}$ ($\alpha \geq 0$). The interaction part of this Hamiltonian has already been studied analytically in Ref. [28], within a canonical-ensemble approach to the equilibrium state of the corresponding d-dimensional model, where it was shown that if the two-body interaction is appropriately scaled, a universal thermodynamical behaviour is achieved for $0 \leq \alpha < d$, e.g., relations involving temperature T, magnetization M, and internal energy U become α-independent in this interval. Apart from this study of the equilibrium state, an investigation of the dynamical behaviour of the above-mentioned Heisenberg model, and particularly, how the QSSs may be affected by the exponent α, has never been addressed in the literature, to our knowledge. In the present work we study this model on a ring, i.e, $d = 1$ with periodic boundary conditions, using molecular-dynamics simulations. We perform a detailed analysis of the QSSs behaviour by varying the energy, number of particles, and range of the interaction, i.e., the exponent α. In the next section we define the model, the appropriate scaling for the interactions, the canonical-ensemble solution, equations of motion, and initial conditions to be used in the molecular-dynamics procedure. In Section III we present the results of our simulations, showing an agreement with some analytical results known in the literature for the equilibrium state, in some particular limits; most importantly, we show the existence of QSSs for energies U below criticality ($U < U_c$). Such QSSs, which were verified herein for initial conditions corresponding to zero magnetization, appear for values of α in the range $0 \leq \alpha < 1$, being characterized by

durations $t_{\rm QSS}$ that increase for increasing values of N, like those found numerically and analytically in previous works of the similar model of XY rotators [9–18, 24, 29, 30]. Finally, in Section IV we present our main conclusions.

II. THE MODEL

First, let us define the model in terms of N localized interacting classical rotators, on a d-dimensional hypercubic lattice, through the Hamiltonian

$$\mathcal{H} = \frac{1}{2}\sum_{i=1}^{N}\mathbf{L}_i^2 + \frac{1}{2\widetilde{N}}\sum_{i=1}^{N}\sum_{\substack{j=1\\ j\neq i}}^{N}\frac{1-\mathbf{S}_i\cdot\mathbf{S}_j}{r_{ij}^{\alpha}} = K + V \ , \tag{1}$$

where $\alpha \geq 0$ and $\mathbf{S}_i$ represents a vector with $n = 3$ components, assigned to the rotator at site i (similar to a classical Heisenberg spin variable), allowed to change its direction continuously inside a 3-dimensional sphere of unity radius, leading to the constraint $\mathbf{S}_i \cdot \mathbf{S}_i = S_i^2 = 1$ $(\forall\ i)$ [1]. Moreover, $\mathbf{L}_i$ depicts the corresponding angular momentum (we are considering moments of inertia equal to unit, so that angular momenta and angular velocities are equivalent quantities). The coupling constants may be identified as $J_{ij} = 1/(\widetilde{N} r_{ij}^{\alpha})$, where r_{ij} measures the (dimensionless) distance between rotators i and j, defined as the minimal one, given that periodic boundary conditions will be considered.

One should notice that the interaction term defined in Eq. (1) is long-ranged for $\alpha \leq d$, in the sense that if $\widetilde{N} \sim \mathcal{O}(1)$ the partition function does not admit a well-defined thermodynamic limit [28], e.g., the internal energy per particle diverges in the limit $N \to \infty$, so that the system is said to be nonextensive [22]. Consequently, in order to calculate the thermodynamic limit adequately whenever $\alpha \leq d$, the quantity $\widetilde{N}$ has to be defined appropriately to ensure a total energy proportional to the system size N. For $\alpha = 0$ this is attained with $\widetilde{N} = N$, the so-called Kac's prescription [4, 5, 17, 28]. For a general $0 \leq (\alpha/d) < \infty$, the extensivity of the Hamiltonian in (1) is achieved through the following choice for $\widetilde{N}$,

$$\widetilde{N} \equiv \frac{1}{N}\sum_{i=1}^{N}\sum_{\substack{j=1\\ j\neq i}}^{N}\frac{1}{r_{ij}^{\alpha}} \ . \tag{2}$$

This may be seen intuitively if we note that for N large, $\widetilde{N} \sim N^{1-\alpha/d}$, if $0 \leq (\alpha/d) < 1$ (hence, $\widetilde{N} \sim N$ for $\alpha = 0$), $\widetilde{N} \sim \ln N$, if $(\alpha/d) = 1$, and $\widetilde{N} \sim 1/(\alpha/d - 1) \sim \mathcal{O}(1)$, if $(\alpha/d) > 1$; therefore, this proposal yields the interaction term in the Hamiltonian (1) proportional to the system size N, for all $\alpha \geq 0$.

The need of the scaling in Eq. (2), for systems characterized by long-range interactions, began to be realized within a generalized ferrofluid model [19] (see also [31]). This proposal was applied successfully to a controllable-range interaction (α-dependent) Curie-Weiss model, where it was shown numerically that by considering such a scaling, the magnetization per particle follows a thermodynamical equation of state, $M = M(T)$, that becomes independent of α in the nonextensive regime [32]. Moreover, applications of this scaling for Lennard-Jones-like systems were carried in Ref. [33]. In addition to the aforementioned works, the correctness of the conjectural scaling of Eq. (2) has been verified in several other systems, suggesting that it should be valid for a wide variety of systems with long-range interactions [22].

[1] This constraint reduces the number of degrees of freedom per particle from three to two.

A systematic analysis of Eq. (2) has been particularly undertaken for the α-XY model [7], whose Hamiltonian is identical to Eq. (1), but $n = 2$, i.e., $\mathbf{S}_i$ is treated as a two-dimensional classical rotator, allowed to change its direction continuously inside a circle of unit radius. For this system, it was shown both analytically [23, 28] and numerically [21, 23, 24, 30] that, for $0 \leq \alpha < d$, the prescription (2) associates to the α-XY model the same thermodynamical behaviour as the one previously known for the case $\alpha = 0$ [6]. Furthermore, the work of Ref. [28] has extended such a result to a general n-dimensional $\mathbf{S}_i$ ($n = 1, 2, \ldots$) unit vector.

Although the model of Eq. (1) has been defined on a d-dimensional hypercubic lattice, from now on we will restrict ourselves to a ring, i.e., a one-dimensional chain with periodic boundary conditions. Based on its successful use for the above-mentioned systems, we will consider the scaling of Eq. (2) for the present problem as well.

A. The Canonical-Ensemble Solution

Within a canonical-ensemble solution, the kinetic term K of the Hamiltonian in Eq. (1) does not bring difficulties in the evaluation of average values. Hence, the nontrivial part for the calculation of equilibrium properties of the Hamiltonian (1) comes from the interaction term V. This term may become troublesome to deal analytically for dimensions $d > 1$, and to our knowledge, it has been investigated analytically only for $d = 1$, i.e., the linear chain, in some particular regimes of α, namely, $\alpha < d$ and $\alpha \to \infty$. The model on an open linear chain with nearest-neighbour interactions (limit $\alpha \to \infty$) was solved exactly in Ref. [1], whose solution is equivalent to the one considering periodic boundary conditions, in the thermodynamic limit [2] (see also Refs. [4, 5, 34]). On the other hand, the fully-coupled limit ($\alpha = 0$) corresponds to the case where the mean-field approach becomes exact, so that the model may be solved through a relatively easy calculation (see, e.g., Ref. [8]). As mentioned above, using the scaling of Eq. (2) the solution for $\alpha = 0$ applies to all $0 \leq \alpha < d$ [28].

Therefore, considering the model of Hamiltonian (1) defined on a ring, i.e., a one-dimensional chain with periodic boundary conditions, the solutions described above may be summarized, yielding for the internal energy and magnetization per particle respectively (we work with units such that $k_{\mathrm{B}} = 1$),

$$U\left(M,T\right) \;=\; \begin{cases} T \;+\; \dfrac{1}{2}\left[1 - L^{2}\left(M/T\right)\right] \;\; ; & \text{if} \;\; 0 \leq \alpha < 1 \;, \\ \\ T \;+\; \dfrac{1}{2}\left[1 - L\left(1/2T\right)\right] \;\; ; & \text{if} \;\; \alpha \to \infty \;, \end{cases} \tag{3}$$

$$M\left(T\right) \;=\; \begin{cases} M = L\left(M/T\right) \;\; ; & \text{if} \;\; 0 \leq \alpha < 1 \;, \\ \\ M = 0 \qquad\quad ; & \text{if} \;\; \alpha \to \infty \;, \end{cases} \tag{4}$$

where $M\left(T\right)$ denotes the modulus of the magnetization vector,

$$\mathbf{M} \;=\; \frac{1}{N}\sum_{i\,=\,1}^{N}\mathbf{S}_i \;. \tag{5}$$

In these equations, $L(x)$ represents the Langevin function,

$$L\left(x\right) \;=\; \coth x \;-\; \frac{1}{x} \;=\; \frac{I_{3/2}\left(x\right)}{I_{1/2}\left(x\right)} \;,$$

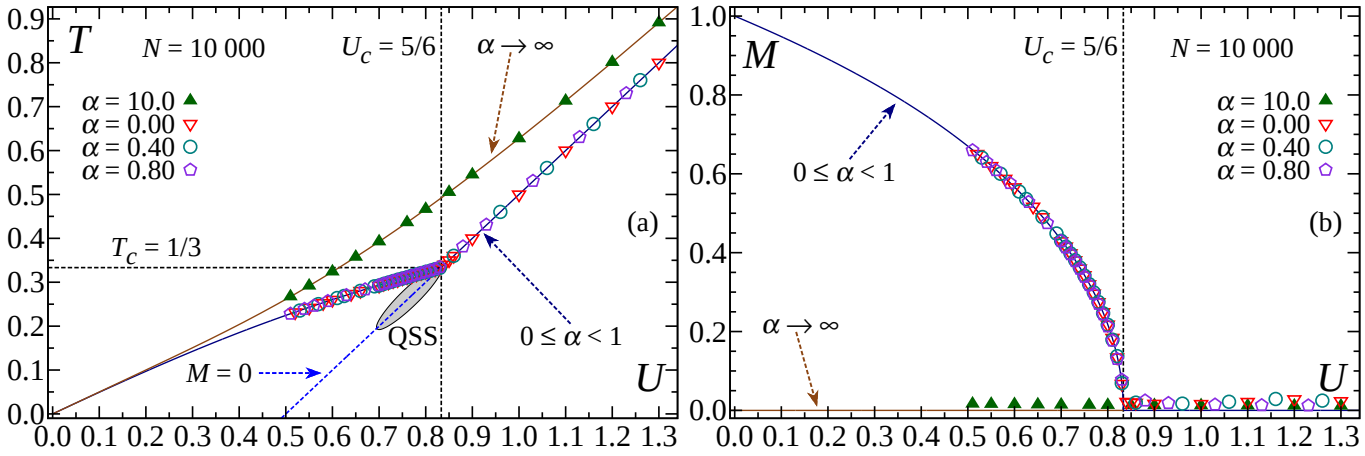

FIG. 1: The good agreement between the analytical results [full lines, cf. Eqs. (3) and (4)] and data from numerical simulations of a system composed by $N = 10\,000$ rotators, in the long-time limit (symbols), is presented for the controllable-range inertial Heisenberg model defined by Eq. (1). (a) The kinetic temperature $T = \langle K(t)\rangle_{\rm time}/N$ (which coincides with the temperature T at equilibrium) versus the internal energy U; (b) The magnetization M versus the internal energy U. In panel (a) (in panel (b)) we compare numerical data, for typical values of α, with the caloric curves (with the magnetization curve) in the cases $0 \leq \alpha < 1$ [8, 28], as well as in the limit $\alpha \to \infty$ [1, 2]. In the former case, one has a second-order phase transition at the critical point $(T_c = 1/3, U_c = 5/6)$ (dashed lines), separating the ferromagnetic $(U < U_c)$ and paramagnetic $(U > U_c)$ phases. The metastable solution corresponding to the quasi-stationary state (QSS) that appears for $U < U_c$, characterized by zero magnetization (shaded region), and presenting a lower kinetic temperature than the corresponding equilibrium solution, is also represented.

and $I_n(x)$ is the modified Bessel function of the first kind.

The analytical results presented above are displayed as solid lines in Fig. 1, where one finds a continuous phase transition separating the ferromagnetic and paramagnetic states for values of α in the interval $0 \leq \alpha < 1$; for $\alpha \to \infty$, there is no phase transition at a finite temperature, so that only the disordered phase with $M = 0$ exists. In the first case, at sufficiently high temperatures (or equivalently, high enough energies), the directions of the $\{\mathbf{S}_i\}$ become randomly distributed, corresponding to the paramagnetic disordered phase, where one has the order parameter $M = 0$. At the fundamental state all spins are parallel, corresponding to the ferromagnetically fully ordered case with $M = 1$. Hence, for all cases $0 \leq \alpha < 1$, in between these two regimes, a continuous phase transition occurs at a critical temperature $T_{\rm c} = 1/3$, with an associated critical energy $U_{\rm c} = 5/6 \approx 0.833$.

B. Equations of Motion

Herein we work with Cartesian components for the spin variables and angular momenta, written respectively as $\mathbf{S}_i = (S_{x_i}, S_{y_i}, S_{z_i})$ and $\mathbf{L}_i = (L_{x_i}, L_{y_i}, L_{z_i})$, yielding 6 variables for each rotator. Hence, the set of $6N$ equations to be solved numerically can be cast in the following form [35],

$$\dot{\mathbf{L}}_i = \mathbf{S}_i \times \left[\frac{1}{\widetilde{N}} \sum_{\substack{j=1 \\ j \neq i}}^{N} \frac{\mathbf{S}_j}{r_{ij}^{\alpha}} \right] , \tag{6a}$$

$$\dot{\mathbf{S}}_i = \mathbf{L}_i \times \mathbf{S}_i , \tag{6b}$$

for $i = 1, 2, \ldots, N$. One notices that, in the particular case $\alpha = 0$, the expression for $\dot{\mathbf{L}}_i$ used in previous works [8, 26] is recovered, namely, $\dot{\mathbf{L}}_i = \mathbf{S}_i \times \mathbf{M}$ [where $\mathbf{M}$ represents the magnetization per particle of Eq. (5)].

It is important to remind that Eqs. (6a) and (6b), written in the Cartesian representation, are not canonical equations of motion, since S_{μ_i} and L_{μ_i} ($\mu = x, y, z$) do not represent canonically conjugate pairs. Alternatively, one could also work along the line of Refs. [27, 36], by using spherical coordinates in order to write the spin variable as $\mathbf{S}_i = (\cos\varphi_i \sin\theta_i, \sin\varphi_i \sin\theta_i, \cos\theta_i)$ and the squared angular momentum in the corresponding Lagrangian as $\mathbf{L}_i^2 = L_{\theta_i}^2 + L_{\varphi_i}^2 / \sin^2\theta_i$. In this representation, one can derive equations of motion through the usual Hamiltonian formalism, where each rotator is characterized by two angles, $\theta_i \in [0, \pi)$ and $\varphi_i \in [0, 2\pi)$, and their canonically conjugate momenta, L_{θ_i} and L_{φ_i}. Although the use of spherical coordinates, instead of the Cartesian ones of Eqs. (6a) and (6b), seems to be a natural way to handle the problem, the denominator $\sin^2\theta_i$ that appears in $\mathbf{L}_i^2$ becomes hard to be tackled numerically. Indeed, as $\sin\theta_i$ approaches zero, one needs to decrease the time step used in the integrations of the equations of motion, in such a way that the computational time may increase substantially. This difficulty has been discussed in the literature by several authors [37–39], where numerical techniques for circumventing it were proposed.

Based on the above-mentioned reasons, herein we shall deal with the equations of motion expressed in terms of Cartesian components, as in Eqs. (6a) and (6b). It is straightforward to verify that, in addition to the total energy, the total angular momentum, $\mathbf{L} = \sum_{i=1}^{N} \mathbf{L}_i$, as well as the norm of each spin, $S_i = [\mathbf{S}_i \cdot \mathbf{S}_i]^{1/2}$, are also integrals of motion. Indeed, evaluating the time derivative of S_i and taking into account that $\dot{\mathbf{S}}_i \perp \mathbf{S}_i$, we get

$$\frac{\mathrm{d}S_i}{\mathrm{d}t} = \frac{\dot{\mathbf{S}}_i \cdot \mathbf{S}_i}{S_i} = 0 \, .$$

Similarly for $\dot{\mathbf{L}}$,

$$\sum_{i=1}^{N} \dot{\mathbf{L}}_i = \left(\sum_{i=1}^{N} \mathbf{S}_i \right) \times \left(\frac{1}{\widetilde{N}} \sum_{j=1}^{N} \frac{\mathbf{S}_j}{r_{ij}^{\alpha}} \right) = 0 \, .$$

It should be stressed that the equation of motion (6a) corresponds precisely to the Euler equation for a linear rigid body of unit length (and unit inertial moments). In such system the angular momentum $\mathbf{L}_i$ is always perpendicular to $\mathbf{S}_i$ (the "molecular" axis), yielding the constraint $\mathbf{L}_i \cdot \mathbf{S}_i = 0$, to be incorporated in the initial state. Once this additional constraint is imposed, it will hold throughout the whole time evolution, since the product $\mathbf{L}_i \cdot \mathbf{S}_i$ is also a constant of motion, as we can verify by using Eqs. (6a) and (6b),

$$\frac{\mathrm{d}}{\mathrm{d}t} \left(\mathbf{L}_i \cdot \mathbf{S}_i \right) = \dot{\mathbf{L}}_i \cdot \mathbf{S}_i + \mathbf{L}_i \cdot \dot{\mathbf{S}}_i = 0 \, . \tag{7}$$

C. Numerical Procedure and Initial Conditions

All our molecular-dynamical simulations were carried for a single copy of the system defined by Eq. (1), considering fixed values of the total number of rotators N and energy per particle U. Since we are applying periodic boundary conditions, the model of Eq. (1) becomes defined on a ring, with r_{ij} corresponding to the minimal dimensionless distance between rotators i and j, taking the values $1, 2, 3 \ldots N/2$, for each rotator i. To integrate the $6N$ equations of motion [Eqs. (6a) and (6b)] we have used a standard fourth-order Runge-Kutta scheme, with an integration step chosen in such a way to yield conservation of the energy per particle within a relative fluctuation smaller than 10^{-5};

this was achieved with a time step typically[2] of $\delta t = 0.02$.

The initial conditions used were such that each angular momentum component L_{μ_i} ($\mu = x, y, z$) was drawn at random from a uniform distribution, and then rescaled to yield zero total angular momentum for the whole system. In what concerns the variables S_{μ_i}, the initial conditions corresponded to those of zero magnetization, achieved numerically as $M \approx 0$ (typically $\sim 10^{-3}$). For this, the components S_{x_i} and S_{y_i} were also drawn at random from a uniform distribution within the interval $[-1, 1]$, whereas the components S_{z_i} were set in such way to preserve the constraint $\mathbf{L}_i \cdot \mathbf{S}_i = 0$ ($\forall i$), i.e., through[3] $S_{z_i} = -\left(L_{x_i} S_{x_i} + L_{y_i} S_{y_i}\right) / L_{z_i}$. This procedure leads to unnormalized spins, which are then normalized by dividing each component by $\sqrt{S_{x_i}^2 + S_{y_i}^2 + S_{z_i}^2}$; finally, all L_{μ_i}'s were rescaled again to obtain precisely the desired total energy U. Consistently with Eqs. (3) and (4), initial configurations with zero magnetization like the one just described above, only applies to a total energy $U > 1/2$.

III. RESULTS

Although we are dealing with three Cartesian components for the angular momenta (L_{x_i}, L_{y_i} and L_{z_i}), due to the constraint $\mathbf{L}_i \cdot \mathbf{S}_i = 0$ only two of these components are independent. Let us then define the instantaneous kinetic temperature as given by $T(t) = K(t)/N$. Since we are working with a single copy of the system defined by Eq. (1), the time average at the equilibrium state should be identified with the thermodynamic temperature, $T = \langle T(t) \rangle_{\text{time}}$, and in a similar way, one has for the equilibrium magnetization, $M = \langle M(t) \rangle_{\text{time}}$. As it will be shown later on, such time averages should be computed after a sufficiently long time, where both $T(t)$ and $M(t)$ fluctuate around the values predicted by Boltzmann-Gibbs (BG) statistical mechanics. In this regime, where ergodicity is expected to hold, time averages and ensemble averages should coincide.

In figure 1 we present results from analytical calculations (full lines) and data from numerical simulations in the long-time limit (symbols), for the controllable-range inertial Heisenberg model of Eq. (1). In figure 1(a) we represent the kinetic temperature versus the internal energy U, whereas in Fig. 1(b) we do the same for the magnetization. As mentioned above, at equilibrium, an average over the quantity $T(t)$ is expected to coincide with the temperature T (obtained from the equipartition theorem), so that for the analytical results presented, the vertical axis of Fig. 1(a) corresponds precisely to the equilibrium temperature T, whereas for the numerical ones, it represents the quantity computed from a time average. All data shown in Fig. 1 for both temperature and magnetization coincide with the analytical results, showing that the equilibrium state considered numerically should be the one predicted by BG theory. The canonical-ensemble solution of the case $\alpha = 0$ (see, e.g., Ref. [8]) is represented by the full line in Fig. 1(a) (usually known as the caloric curve), presenting a discontinuity in its slope at the critical point ($T_c = 1/3, U_c = 5/6$), where the magnetization becomes zero. According to Ref. [28], the equilibrium analytical solution of the case $\alpha = 0$ should apply to any $0 \leq \alpha < 1$, so that the corresponding full lines in Figs. 1(a) and (b) hold for any α in this range. Such a universal behaviour was verified numerically for the α-XY model [21, 23, 24, 30],

[2] A substantial gain in computational time was obtained, in the simulations with $\alpha \neq 0$ and larger values of N, by using a Fast-Fourier-Transform algorithm. To implement this technique we have used the FFTW library http://www.fftw.org.

[3] It should be mentioned that this constraint was not used in Refs. [8, 26], so that $\mathbf{L}_i \cdot \mathbf{S}_i = \delta_i$ ($\delta_i \in [-1, 1]$) in these works, at the beginning of the simulations. However, it was verified numerically that δ_i was also a constant of motion, in such a way that Eq. (7) remained true ($\forall i$).

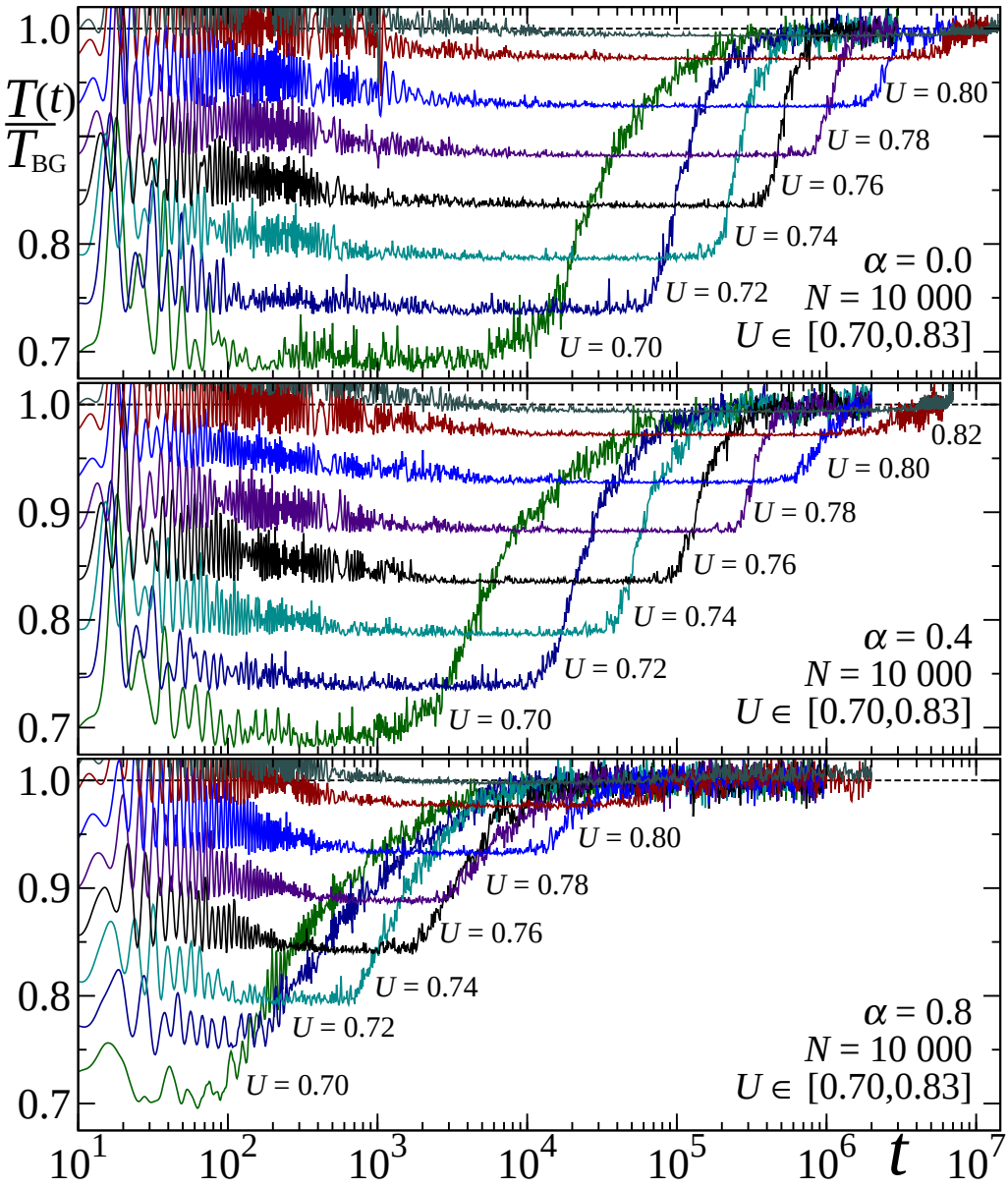

FIG. 2: Time evolution of the dimensionless quantity $T(t)/T_{\rm BG}$ for typical values of the total energy U ($U < U_{\rm c}$), for a single copy of $N = 10\,000$ Heisenberg rotators, in the cases $\alpha = 0.0, 0.4$, and 0.8 (from top to bottom). For each value of U, the corresponding equilibrium temperature $T_{\rm BG}$ is obtained from the caloric curve in Fig. 1. The time is also dimensionless and each unit of (physical) time t corresponds to 50 iterations of the equations of motion.

and it is now established herein for the Heisenberg model, as displayed in Fig. 1 for typical values of $0 \leq \alpha < 1$. For completeness, in Fig. 1(a) we also present the solution corresponding to the quasi-stationary state (QSS) hat appears for $U < U_c$, characterized by zero magnetization, leading to $T = U - 1/2$, and presenting a lower kinetic temperature than the corresponding equilibrium solution. It was essentially within the energy range $0.70 \lesssim U < U_c = 5/6$ that QSSs have been investigated within the present numerical investigation. In the limit $\alpha \to \infty$ our model recovers the nearest-neighbour-interaction inertial Heisenberg model on a linear chain, for which the interaction part was solved exactly in Refs. [1, 2], and shown to present zero magnetization for all $T > 0$; consequently, its caloric curve exhibits the smooth behaviour indicated in Fig. 1(a). In this case, our simulations for $\alpha = 10$ are in full agreement with the results of the analytical solutions.

In figure 2 we exhibit the time evolution of $T(t)$ (conveniently rescaled in each case by the cor-

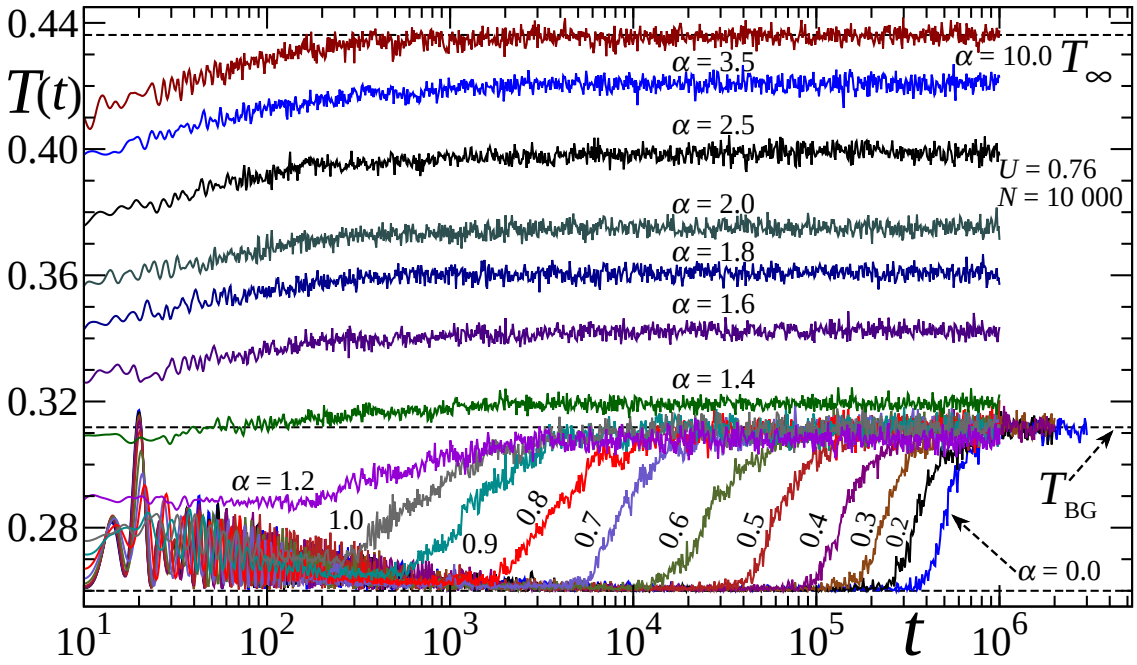

FIG. 3: Time evolution of the kinetic temperature $T(t) = K(t)/N$ for a single realization of $N = 10\,000$ Heisenberg rotators defined by Eq. (1), with a total energy $U = 0.76$, and several values of the interaction-range parameter α. The upper horizontal dashed line, at $T_\infty \approx 0.4362$, represents the Boltzmann-Gibbs (BG) equilibrium temperature of the corresponding $\alpha \to \infty$ model [cf. Eq. (3)]. The dashed horizontal line at $T_{\rm BG} \approx 0.3118$ indicates the BG equilibrium temperature for $0 \leq \alpha < 1$ [see Eqs. (3) and (4)], whereas the lower horizontal line, at $T = U - 1/2 = 0.26$, corresponds to the QSS temperature characterized by zero magnetization. In the range $1 \leq \alpha < \infty$, no analytical solution is available, as far as we know. The time is dimensionless and each unit of (physical) time t corresponds to 50 iterations of the equations of motion.

responding equilibrium temperature $T_{\rm BG}$) for typical values of energies, $U < U_{\rm c} = 5/6 \approx 0.833$, and $\alpha = 0.0, 0.4$, and 0.8. Simulations were carried for a single copy of $N = 10\,000$ rotators, considering the above-defined initial conditions, for sufficiently long times (up to times slightly larger than $t = 10^7$ in some cases). For all energies investigated, in the range $0.70 \leq U \leq 0.83$, we have verified the existence of QSSs and after these, a crossover is observed to a state whose temperature and magnetization coincide with those obtained analytically within BG statistical mechanics. For a given value of α one has that: (i) The lower energies have produced QSSs with smaller durations $t_{\rm QSS}$, and one observes that $t_{\rm QSS}$ increases substantially as one approaches the critical energy; (ii) The gaps separating $T(t)$ of these QSSs and their corresponding values of equilibrium temperatures $T_{\rm BG}$ are larger for smaller energies, dropping to zero as $U \to U_c$. On the other hand, for a fixed total energy, higher values of α yield smaller $t_{\rm QSS}$, and it will be shown later on that these durations tend to zero as $\alpha \to 1$. Therefore, the QSSs disappear in both limits $U \to U_c$ and $\alpha \to 1$. The existence of QSSs for energies below, but sufficiently close to U_c, is well known to occur in the HMF and α-XY (with $0 < \alpha < 1$) models, and it has been found analytically and numerically by many authors [9–18, 24, 29, 30]. Moreover, the most interesting characteristic of such states concerns an increase in their lifetime with the total number of rotators N; this property will also be verified for the present model.

The QSSs shown in Fig. 2 appear throughout the whole range $0 \leq \alpha < 1$, as exhibited in Fig. 3 for several values of α. Each case corresponds to molecular-dynamics simulations of a single realization of $N = 10\,000$ Heisenberg rotators defined by Eq. (1), with a total energy $U = 0.76$. One sees that the lifetime of these QSSs decrease for increasing values of α in the range $0 \leq \alpha < 1$ and that all

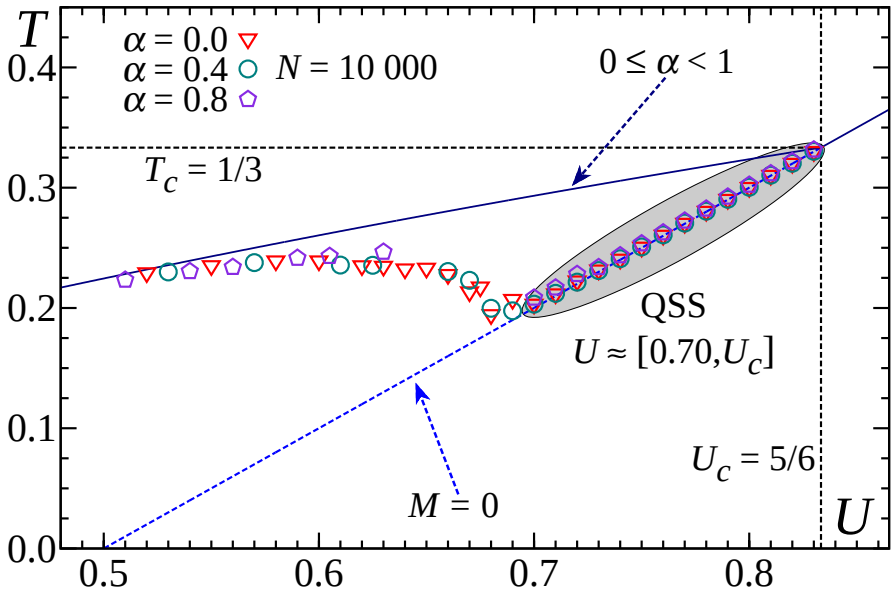

FIG. 4: Part of the caloric curve for the cases $0 \leq \alpha < 1$ [cf. Fig. 1(a)] is exhibited for energies $U \leq U_c$ (full line). The range of energies over which QSSs were verified numerically is shown for both zero magnetization (dashed line), as well as for $M > 0$. The symbols correspond to data associated with the kinetic temperatures of the QSSs, obtained from numerical simulations for a single copy of a system composed by $N = 10\,000$ rotators, in the cases $\alpha = 0.0, 0.4$, and 0.8.

QSSs occur at a kinetic temperature corresponding to zero magnetization (or slightly larger than zero), i.e., $T \gtrsim U - 1/2 = 0.26$. After these QSSs, the system approaches the BG equilibrium temperature ($T_{\rm BG} \approx 0.3118$), associated to its energy through the caloric curve of Fig. 1. At $\alpha \approx 1$ one notices a crossover from the existence of these metastable states to a smooth gradual increase in the kinetic temperature, such that for $\alpha > 1$ there is no clear evidence of QSSs. Finally, for a sufficiently high value of α (e.g., $\alpha = 10$), the long-time behaviour of the kinetic temperature $T(t)$ gradually approaches the BG equilibrium temperature of the corresponding $\alpha \to \infty$ model, i.e., the nearest-neighbour-interaction model ($T_\infty \approx 0.4362$). Our numerical results however do not exclude a possible finite-size dependence of these short-lived QSSs for $\alpha \gtrsim 1$, as already found in the α-XY case [40]. However, no dependence on N is expected for $\alpha \gg 1$, since the interaction potential becomes effectively short range in this limit.

An important question concerns the range of energies over which the above-mentioned QSSs exist. In figure 4 we present part of the caloric curve for $0 \leq \alpha < 1$, corresponding to energies $U \leq U_c$ (full line). Numerical simulations for a single copy of $N = 10\,000$ rotators, in the cases $\alpha = 0.0, 0.4$, and 0.8, show that the QSSs characterized by $M = 0$ (symbols along the dashed line) exist within the range $0.70 \lesssim U < U_c$, in agreement with the results of Fig. 2. However, as one goes further below the critical point, roughly for $0.50 < U < 0.70$, QSSs are still found numerically, although characterized by finite values of magnetization, in spite of the initial conditions of zero magnetization considered. Such states are understood due to the prevalence of the ferromagnetic couplings for sufficiently low values of U, and they may be observed more clearly in the case $\alpha = 0.0$, being sometimes difficult to be identified for higher values of α (e.g., $\alpha = 0.80$). It should be noticed that within a small energy range (typically $U \lesssim 0.70$), the QSSs yield a negative microcanonical specific heat. Although this represents a well-known feature for the HMF model (see discussion in Ref. [15]), it is the first time that such a result is verified for a system of Heisenberg rotators, to our knowledge. The numerical data of Fig. 4 suggests that a negative specific heat should occur for $0 \leq \alpha < 1$.

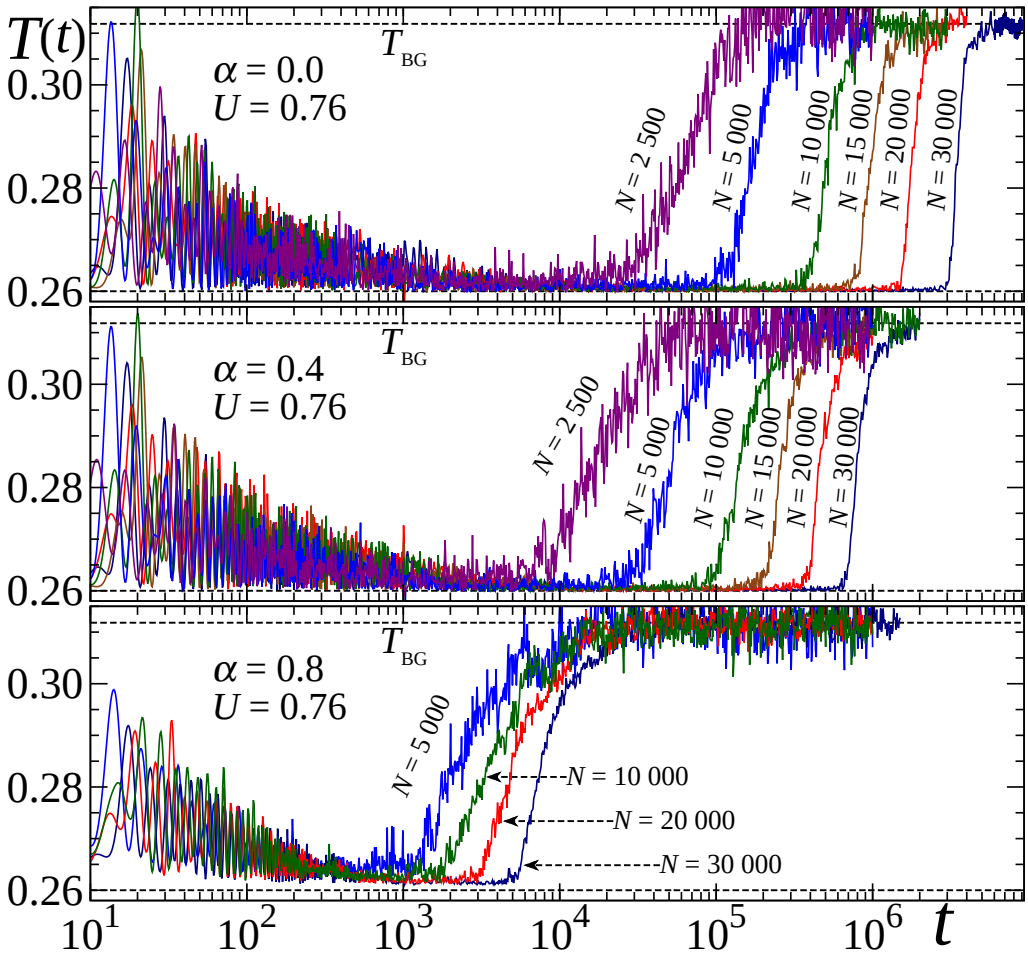

FIG. 5: Typical QSSs presented in Figs. 2 and 3 are analysed for varying system sizes, showing an increase in their lifetime $t_{\rm QSS}$ as N increases.

The most interesting feature of the QSSs presented in Figs. 2 and 3 concerns an increase in $t_{\rm QSS}$ for increasing N, as shown in Fig. 5, where we analyse the QSSs for an energy $U = 0.76$ in the cases $\alpha = 0.0, 0.4$, and 0.8, by varying the system sizes. It should be mentioned that, in order to identify QSSs clearly within the present approach, we had to simulate systems with sufficiently high values of N (essentially, $N = 2\,500$ or higher). Hence, in Fig. 5 such a behaviour is presented for typical values of N in the range from $N = 2\,500$ up to $N = 30\,000$, for the smaller values of α (i.e., $\alpha = 0.0$ and 0.4); however, in the case $\alpha = 0.8$ the observation of QSSs becomes more difficult, in such a way that one needs to simulate larger values of N (e.g., $N = 5\,000$ or higher) for this purpose. The growth of $t_{\rm QSS}$ for increasing N represents a well-known feature in models of rotators, like the HMF and α-XY (with $0 < \alpha < 1$) models [9–17, 24, 29, 30], as well as the inertial Heisenberg model [8, 26, 27], yielding significant physical consequences, some of them directly related to the applicability of BG statistical mechanics. More specifically, the order in which the thermodynamic limit ($N \to \infty$) and the infinite-time limit ($t \to \infty$) are considered becomes mostly relevant in the present case, in such a way that if the thermodynamic limit is carried first, one should remain in a QSS forever. This may be viewed as a breakdown of ergodicity, with the system being trapped in a QSS, never reaching the BG equilibrium state; consequently, time averages and ensemble averages do not coincide, violating a basic assumption of BG statistical mechanics. The QSS represents the final state in this case; whether it should be interpreted as a truly equilibrium thermodynamical one represents an important question beyond the scope of the present work.

Herein we have defined the duration $t_{\rm QSS}$ of a given QSS (e.g., those exhibited in Fig. 5), as the

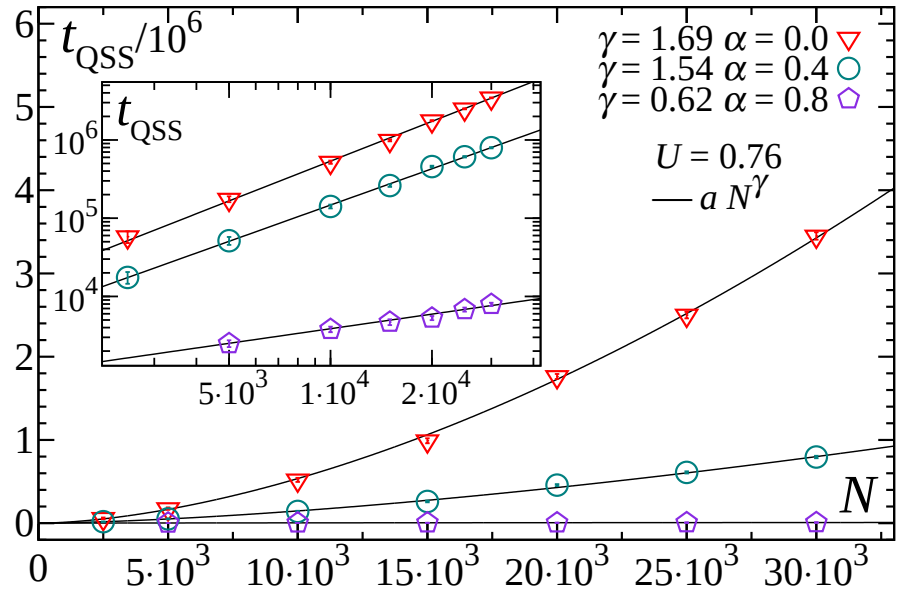

FIG. 6: The growth of the lifetime of the QSSs ($t_{\rm QSS}$) with respect to the size of the system is presented, for a fixed energy ($U = 0.76$) and three typical values of α ($\alpha = 0.0, 0.4$, and 0.8). Symbols correspond to data from numerical simulations, whereas full lines stand for the fits proposed. In the inset we exhibit the same data in a log-log representation.

time at which $T(t)$ presents its halfway between the values at the QSS and its corresponding $T_{\rm BG}$. The fact that we are computing this time interval starting from $t = 0$, including a short transient regime before reaching the QSS, does not affect our final results, since this small transient becomes negligible in the final computation of $t_{\rm QSS}$, for sufficiently large values of N. According to this, the growth of $t_{\rm QSS}$ with the total number of rotators N, for a given energy ($U = 0.76$) and three typical values of α ($\alpha = 0.0, 0.4$, and 0.8), is exhibited in Fig. 6. In the three cases investigated, these behaviours are fitted by power laws, $t_{\rm QSS} \sim N^{\gamma}$ (as shown in the respective inset, where the same data is presented in a log-log representation), with the exponent γ decreasing as α increases, e.g., $\gamma \approx 1.69$ ($\alpha = 0.0$), $\gamma \approx 1.54$ ($\alpha = 0.4$), and $\gamma \approx 0.62$ ($\alpha = 0.8$). In the first case, our estimate agrees with the one of Ref. [27] (see also [41]), where $\gamma \approx 1.70$ was computed. Curiously, such an estimate has also been found numerically for QSSs of the HMF model, with similar initial conditions (zero magnetization) [10], being supported through analytical approaches in Ref. [16]. One should mention that in the case $\alpha = 0.8$ the QSSs are more difficult to be observed, appearing only for sufficiently high values of N, such that data points for smaller N are not exhibited. In spite of such difficulties, our simulations suggest that one should have $\gamma \to 0$ in the limit $\alpha \to 1$. Although relevant, it is not possible to propose a particular scaling behaviour describing the decrease of γ with respect to α, on the basis of the present numerical simulations. Such a scaling deserves further computational efforts, from which one could obtain a larger number of data points for an appropriate plot of γ versus α (see, e.g., Ref. [42] for the XY case).

The behaviours of the duration $t_{\rm QSS}$ of the present QSSs with respect to the total energy U, as well as its decrease with the parameter α are presented in Fig. 7. In figure 7(a) we exhibit data of simulations of $N = 10\,000$ rotators, for three values of α ($\alpha = 0.0, 0.4$, and 0.8), varying the energy in the range $0.70 \leq U < U_c$. These results show that $t_{\rm QSS}$ grows exponentially for increasing U in this range, as can be seen more clearly through the log-linear representation in the inset. Although $t_{\rm QSS}$ may become very large as $U \to U_c$, from the plots of Fig. 2 one sees that the gap between the kinetic temperature of each QSS and the equilibrium state, represented by $T_{\rm BG}$,

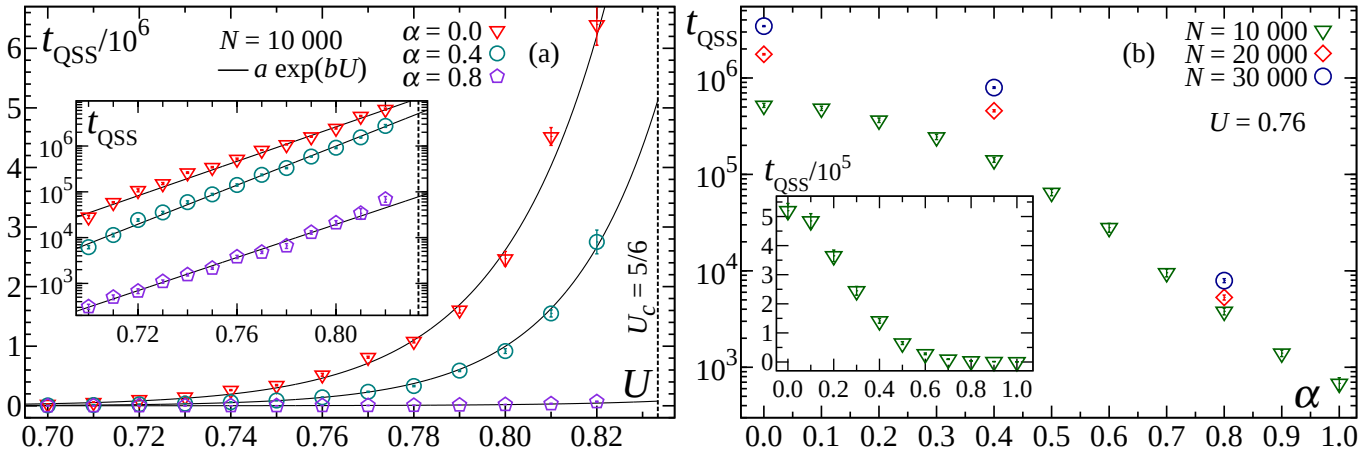

FIG. 7: Behaviours of the lifetime of the QSSs ($t_{\rm QSS}$), with respect to the energy U and to the interaction-range parameter α, are shown. (a) Fixed number of rotators ($N = 10\,000$), three typical values of α ($\alpha = 0.0, 0.4$, and 0.8), varying the energy in the range $0.70 \leq U < U_c$; the same data are exhibited in a log-linear representation in the inset. (b) Fixed energy ($U = 0.76$), three values for the total number of rotators ($N = 10\,000, 20\,000$, and $30\,000$), varying α in the range $0 \leq \alpha \leq 1$; the data for $N = 10\,000$ are exhibited in a linear-linear representation in the inset. Symbols correspond to data from numerical simulations of a single copy of the Hamiltonian in Eq. (1), whereas full lines stand for the fits proposed.

decreases as U approaches U_c. Hence, in this case, the QSSs disappear by means of the difference between these two quantities, which goes to zero as $U \to U_c$, so that for $U \gtrsim U_c$ one finds no QSSs. The dependence of $t_{\rm QSS}$ on the interaction-range parameter α ($0 \leq \alpha \leq 1$) is presented in Fig. 7(b), where we exhibit data of simulations for the energy $U = 0.76$ and three values for the total number of rotators ($N = 10\,000, 20\,000$, and $30\,000$). In the log-linear representation, one sees that these results do strongly depend on N, although they are all suggestive that $t_{\rm QSS} \to 0$ as $\alpha \to 1$; more particularly, the linear-linear representation of the inset indicates this tendency more clearly in the case $N = 10\,000$.

IV. CONCLUSIONS

We have carried molecular-dynamics simulations on a one-dimensional Hamiltonian system, composed by N classical localized Heisenberg rotators on a ring. We have considered the two-body interaction characterized by a distance r_{ij} between rotators at sites i and j, decaying with the distance r_{ij} as a power law, $1/r_{ij}^{\alpha}$ ($\alpha \geq 0$). In this way, one may control the range of the interactions by changing the parameter α, and specially, two well-known cases may be recovered, namely, the fully-coupled (i.e., mean-field limit) and nearest-neighbour-interaction models, in the limits $\alpha = 0$ and $\alpha \to \infty$, respectively. For the first time in the literature, we have numerically established the validity of the correct scaling for spin dimensionality $n > 2$. Considering this scaling, one obtains the same thermodynamical behaviour for any α in the range $0 \leq \alpha < 1$, as analytically predicted in Ref. [28].

We have investigated the dynamics of the model by following the time evolution of a single copy of rotators, for energies U below its critical value ($U < U_c$), considering initial conditions corresponding to zero magnetization. Analogously to what happens for the similar model of XY rotators, we have verified the existence of quasi-stationary states (QSSs) for values of α in the range $0 \leq \alpha < 1$. But, in contrast to the XY rotators, the allowed number of initial conditions of the present model

is substantially larger. The particular types of initial conditions that will lead the system to robust QSSs was discussed, representing a very relevant matter for further analytical investigations. For a given energy U, our numerical analysis indicated that the durations $t_{\rm QSS}$ grow by increasing N, following a power law, $t_{\rm QSS} \sim N^{\gamma}$, where the exponent γ gets reduced for increasing values of α in the range $0 \leq \alpha < 1$; particularly, our results suggest that $\gamma \to 0$ as $\alpha \to 1$. The relevance of establishing the growth of $t_{\rm QSS}$ with N accurately, achieved herein by considering sufficiently large values of N, may be assessed if one takes into account the fact that in spite of the large amount of effort dedicated to the α-XY model, this matter is still controversial for this system (see, e.g., Refs. [16, 18]). The particular scaling behaviour, describing the decrease of γ with respect to α, requires further computational efforts and is left for future investigations. Moreover, for the initial conditions and energy range considered, we have shown that the duration of the QSSs grows exponentially with the energy, $t_{\rm QSS} \sim \exp(bU)$, for N and α fixed. Our simulations have indicated that the gaps separating the kinetic temperature of these QSSs and their corresponding equilibrium temperatures $T_{\rm BG}$ become larger for smaller energies, dropping to zero as $U \to U_c$. In this way, the QSSs disappear by means of the difference between these two quantities, which goes to zero as $U \to U_c$, so that for $U \gtrsim U_c$ one finds no QSSs.

We have found QSSs over a wide range of energies, typically for $0.50 < U < U_c$ ($U_c = 5/6$), although these states presented zero magnetization throughout a smaller interval, $0.70 \lesssim U < U_c$. It should be mentioned that we have chosen to explore more deeply the QSSs associated with a given value of energy ($U = 0.76$), where such states could be observed easily through simulations of a single copy of rotators. However, the results presented herein for this particular energy should be valid for any similar QSS (characterized by zero magnetization) in the range $0.70 \lesssim U < U_c$. By going further below the critical point, roughly for $0.50 < U < 0.70$, QSSs were still found numerically, but in contrast to the above-mentioned ones, they are characterized by finite values of magnetization, in spite of the initial conditions of zero magnetization considered. Within a small energy range (typically $U \lesssim 0.70$), the numerical data of the kinetic temperature of these QSSs versus U yielded a negative microcanonical specific heat. Although this represents a well-known feature for the HMF model, it is the first time that such a result has been verified for a system of Heisenberg rotators, to our knowledge.

The particular case $\alpha = 0.0$ of the present analysis (carried herein for the Cartesian components of angular momenta and spin variables), coincides precisely with the one of Ref. [27], which have considered angular variables and their corresponding canonically-conjugated angular momenta. Herein, we have extended these results for power-law decaying interactions among spin variables, by investigating situations characterized by $\alpha > 0$, showing that interesting QSSs appear for any α in the range $0 \leq \alpha < 1$. Due to the wide diversity of possibilities for initial conditions in both spins and angular momenta in the present model, investigations for QSSs under initial conditions different from the ones considered herein would be highly desirable.

Acknowledgments

We acknowledge useful conversations with C. Tsallis, M. Jauregui, S. T. O. Almeida, M. S. Ribeiro, G. A. Casas, E. R. P. Novais, and F. T. L. Germani. We have benefited from partial financial supports by

CNPq, Faperj and Capes (Brazilian funding agencies).

[1] T. Nakamura, *Statistical theory of hindered rotation in molecular crystals*, J. Phys. Soc. Jpn. **7**, 264–269 (1952); M. E. Fisher, *Magnetism in one-dimensional systems–The Heisenberg model for infinite spin*, Am. J. Phys. **32**, 343–346 (1964).

[2] G. S. Joyce, *Classical Heisenberg model*, Phys. Rev. **155**, 478–491 (1967).

[3] H. E. Stanley, *Exact solution for a linear chain of isotropically interacting classical spins of arbitrary dimensionality*, Phys. Rev. **179**, 570–577 (1969).

[4] H. E. Stanley, *Introduction to phase transitions and critical phenomena* (Oxford University Press, New York, 1971).

[5] C. J. Thompson, *Classical equilibrium statistical mechanics* (Oxford University Press, Oxford, 1988).

[6] M. Antoni and S. Ruffo, *Clustering and relaxation in Hamiltonian long-range dynamics*, Phys. Rev. E **52**, 2361–2374 (1995).

[7] C. Anteneodo and C. Tsallis, *Breakdown of exponential sensitivity to initial conditions: Role of the range of interactions*, Phys. Rev. Lett. **80**, 5313–5316 (1998).

[8] F. D. Nobre and C. Tsallis, *Classical infinite-range-interaction Heisenberg ferromagnetic model: Metastability and sensitivity to initial conditions*, Phys. Rev. E **68**, 036115 (2003).

[9] V. Latora, A. Rapisarda, and C. Tsallis, *Non-Gaussian equilibrium in a long-range Hamiltonian system*, Phys. Rev. E **64**, 056134 (2001).

[10] Y. Y. Yamaguchi, J. Barré, F. Bouchet, T. Dauxois, and S. Ruffo, *Stability criteria of the Vlasov equation and quasi-stationary states of the HMF model*, Physica A **337**, 36–66 (2004).

[11] A. Pluchino, V. Latora, and A. Rapisarda, *Glassy dynamics in the HMF model*, Physica A **340**, 187–195 (2004); *Effective spin–glass Hamiltonian for the anomalous dynamics of the HMF model*, Physica A **370**, 573–584 (2006); *Metastable states, anomalous distributions and correlations in the HMF model*, Physica D **193**, 315–328 (2004).

[12] V. Latora, A. Rapisarda, and S. Ruffo, *Lyapunov instability and finite size effects in a system with long-range forces*, Phys. Rev. Lett. **80**, 692–695 (1998); *Chaos and statistical mechanics in the Hamiltonian mean field model*, Physica D **131**, 38–54 (1999).

[13] L.G. Moyano and C. Anteneodo, *Diffusive anomalies in a long-range Hamiltonian system*, Phys. Rev. E **74**, 021118 (2006).

[14] A. Pluchino, A. Rapisarda, and C. Tsallis, *Nonergodicity and central-limit behavior for long-range Hamiltonians*, Europhys. Lett. **80**, 26002 (2007); *A closer look at the indications of q-generalized central limit theorem behavior in quasi-stationary states of the HMF model*, Physica A **387**, 3121–3128 (2008).

[15] P.-H. Chavanis and A. Campa, *Inhomogeneous Tsallis distributions in the HMF model*, Eur. Phys. J. B **76**, 581–611 (2010); A. Campa and P.-H. Chavanis, *Caloric curves fitted by polytropic distributions in the HMF model*, Eur. Phys. J. B **86**, 170 (2013).

[16] W. Ettoumi and M.-C. Firpo, Action diffusion and lifetimes of quasistationary states in the Hamiltonian mean-field model. Phys. Rev. E **87**, 030102 (2013).

[17] A. Campa, T. Dauxois, and S. Ruffo, *Statistical mechanics and dynamics of solvable models with long-range interactions*, Phys. Rep. **480**, 57–159 (2009).

[18] T. M. Rocha Filho, M. A. Amato, A. E. Santana, A. Figueiredo and J. R. Steiner, *Dynamics and physical interpretation of quasistationary states in systems with long-range interactions*, Phys. Rev. E **89** 032116 (2014); T. M. Rocha Filho, A. E. Santana, M. A. Amato and A. Figueiredo, *Scaling of the dynamics of homogeneous states of one-dimensional long-range interacting systems*, Phys. Rev. E **90** 032133 (2014).

[19] P. Jund, S. G. Kim, and C. Tsallis, *Crossover from extensive to nonextensive behavior driven by long-range interactions*, Phys. Rev. B **52**, 50–53 (1995).

[20] A. Campa, A. Giansanti, D. Moroni, and C. Tsallis, *Classical spin systems with long-range interactions: universal reduction of mixing*, Phys. Lett. A **286**, 251–256 (2001).

[21] F. Tamarit and C. Anteneodo, *Rotators with long-range interactions: Connection with the mean-field*

approximation, Phys. Rev. Lett. **84**, 208–211 (2000).

[22] C. Tsallis, *Introduction to nonextensive statistical mechanics – Approaching a complex world* (Springer, New York, 2009).

[23] A. Campa, A. Giansanti, and D. Moroni, *Canonical solution of a system of long-range interacting rotators on a lattice*, Phys. Rev. E **62**, 303–306 (2000).

[24] L. J. L. Cirto, V. R. V. Assis, and C. Tsallis, *Influence of the interaction range on the thermostatistics of a classical many-body system*, Physica A **393**, 286–296 (2014).

[25] M.-C. Firpo and S. Ruffo, *Chaos suppression in the large size limit for long-range systems*, J. Phys. A **34**, L511 (2001); C. Anteneodo and R. O. Vallejos, *Scaling laws for the largest Lyapunov exponent in long-range systems: A random matrix approach*, Phys. Rev. E **65**, 016210 (2001).

[26] F. D. Nobre and C. Tsallis, *Metastable states of the classical inertial infinite-range-interaction Heisenberg ferromagnet: role of initial conditions*, Physica A **344**, 587–594 (2004).

[27] S. Gupta and D. Mukamel, *Quasistationarity in a model of long-range interacting particles moving on a sphere*, Phys. Rev. E **88**, 052137 (2013).

[28] A. Campa, A. Giansanti, and D. Moroni, *Canonical solution of classical magnetic models with long-range couplings*, J. Phys. A–Math. Gen. **36**, 6897 (2003).

[29] A. Campa, A. Giansanti, and D. Moroni, *Metastable states in a class of long-range Hamiltonian systems*, Physica A **305**, 137–143 (2002).

[30] A. Giansanti, D. Moroni, and A. Campa, *Universal behavior in the static and dynamic properties of the α-XY model*, Chaos Soliton. Fract. **13**, 407–416 (2002).

[31] C. Tsallis, *Nonextensive thermodynamics and fractals*, Fractals **03**, 541–547 (1995).

[32] S. A. Cannas and F. A. Tamarit, *Long-range interactions and nonextensivity in ferromagnetic spin models*, Phys. Rev. B **54**, R12661–R12664 (1996); L. C. Sampaio, M. P. de Albuquerque, and F. S. de Menezes, *Nonextensivity and Tsallis statistics in magnetic systems*, Phys. Rev. B **55**, 5611–5614 (1997).

[33] J. R. Grigera, *Extensive and non-extensive thermodynamics. a molecular dynamic test*, Phys. Lett. A **217**, 47–51 (1996); S. Curilef and C. Tsallis, *Critical temperature and nonextensivity in long-range interacting Lennard–Jones-like fluids*, Phys. Lett. A **264**, 270–275 (1999).

[34] J. D. Parsons, *Linear chain of classical spins with arbitrary isotropic nearest-neighbor interaction*, Phys. Rev. B **16**, 2311–2312 (1977).

[35] D. C. Rapaport and D. P. Landau, *Critical dynamics of a dynamical version of the classical Heisenberg model*, Phys. Rev. E **53**, 4696–4702 (1996).

[36] D. T. Robb, L. E. Reichl, and E. Faraggi, *Simulation of hysteresis in magnetic nanoparticles with Nosé thermostating*, Phys. Rev. E **67**, 056130 (2003).

[37] J. Barojas, D. Levesque, and B. Quentrec, *Simulation of diatomic homonuclear liquids*, Phys. Rev. A **7**, 1092–1105 (1973).

[38] D. J. Evans, *On the representation of orientation space*, Mol. Phys. **34**, 317–325 (1977); D. J. Evans and S. Murad, *Singularity free algorithm for molecular dynamics simulation of rigid polyato*, Mol. Phys. **34**, 327–331 (1977).

[39] M. P. Allen and D. J. Tildesley, *Computer Simulation of Liquids* (Oxford University Press, Oxford, 1987).

[40] A. Turchi, D. Fanelli and X. Leoncini, *Existence of quasi-stationary states at the long range threshold*, Commun. Nonlinear Sci. Numer. Simulat. **16** 4718–4724 (2011); W. Ettoumi and M.-C. Firpo, *Stochastic treatment of finite-N effects in mean-field systems and its application to the lifetimes of coherent structures*, Phys. Rev. E **84** 030103 (2011).

[41] S. Gupta and D. Mukamel, *Quasistationarity in a model of classical spins with long-range interactions*, J. Stat. Mech.: Theor. Exp. P03015 (2011).

[42] R. Bachelard and M. Kastner, *Universal Threshold for the Dynamical Behavior of Lattice Systems with Long-Range Interactions*, Phys. Rev. Lett. 170603 **110** (2013).